Cyclohexane Dehydrogenation and H_2 Adsorption on Pt Particles on ZnO(0001)−O

Ann W. Grant,† Lien T. Ngo, Karsten Stegelman, and Charles T. Campbell*

Department of Chemistry, University of Washington, Seattle, Washington 98195-1700

Received: August 20, 2002; In Final Form: November 27, 2002

The dehydrogenation of cyclohexane on Pt/ZnO(0001)−O model catalysts was studied with temperature programmed desorption (TPD), low-energy ion scattering spectroscopy, and X-ray photoelectron spectroscopy. Vapor-deposited Pt grows on this O-terminated ZnO face as 2-dimensional (2D) islands at low coverage, and later as 3D particles. The reactivity of these Pt nanoparticles toward H_2 and *c*-C_6D_{12} was studied versus Pt coverage, which controls their lateral dimension and then their thickness. Dissociatively adsorbed H_2 gives an H_2 TPD peak at ∼330 K from Pt particles, nearly independent of their size or thickness. The initial sticking probability for *c*-C_6D_{12} at 170 K is higher on Pt particles than on ZnO. Adsorbed *c*-C_6D_{12} on this ZnO surface desorbs intact at ∼220 K. When *c*-C_6D_{12} is adsorbed on Pt islands, some of it desorbs molecularly at ∼250 K, but most of it (>60%) dehydrogenates. The dehydrogenation pathway produces two main D_2 TPD regions: ∼300−400 K, peaking at ∼370 K, and 450−750 K, peaking at ∼580 K. This is similar to the dominant H_2 peaks seen from low-index faces of Pt crystals because of dehydrogenation of adsorbed *c*-C_6H_{12} to adsorbed benzene plus H (370 K) and further dehydrogenation of benzene to adsorbed C_2H (∼560 K) and finally graphitic carbon (600−750 K). The ∼580 K peak is broadened considerably on particles compared to low-index faces. The probability for *c*-C_6D_{12} dehydrogenation is much higher on Pt particles than on Pt(111), especially when the particles are 2D. The probability for loss of product D (or H) into the bulk of the ZnO is high at lower temperature, which decreases the apparent intensity ratio of the two main D_2 TPD peak regions (370 K: 580 K and above) relative to the stoichiometric 1:1 ratio seen for Pt(111).

1. Introduction

The dehydrogenation of cyclohexane to benzene on Pt catalysts as a prototypical hydrocarbon reforming reaction was first recognized by Zelinskii in 1911[1] and introduced commercially in 1949. The typical hydrocarbon reforming catalysts consists of ∼1 nm Pt particles supported on alumina.[1]

This paper examines the dehydrogenation of cyclohexane and the adsorption of H_2 over model catalysts prepared by vapor depositing Pt onto ZnO(0001)−O. This ZnO(0001)−O surface terminates in a hexagonal array of oxygen anions. Thus, this is a very simple model oxide surface, uncomplicated by reactivity because of coordinatively unsaturated metal cations (except at defects). As we show below, films prepared by the vapor deposition of Pt on ZnO(0001)−O follow a 2D island growth mode, where a distinct transition between 2D and 3D Pt islands is seen by LEIS at ∼0.5 ML. Thus, Pt/ZnO(0001)−O provides an interesting model oxide-supported Pt catalyst, where the reactivity of Pt particles that are only one atom thick can be compared to thicker particles. Because the lateral size of the 2D islands increases with coverage up to 0.5 ML, the effect of this dimension can also be tested.

Platinum on ZnO and/or Pt−Zn combinations on other oxides are also active catalysts for a number of different reactions, such as highly selective dehydrogenation of alkanes,[2,3] selective dehydrogenation of α,β-unsaturated aldehydes,[4] vapor-phase hydrogenation of crotonaldehyde to crotyl alcohol,[5] methanol steam reforming to CO_2 and H_2,[6,7] and selective methanol dehydrogenation to methyl formate.[7,8]

Cyclohexane dehydrogenation has been studied extensively on Pt single crystals using surface science techniques.[9−28] Cyclohexane adsorbs molecularly on Pt(111) at 100 K with C_{3v} symmetry.[18,19,10] At ∼240 K, some of the cyclohexane desorbs and some dehydrogenates to a *c*-C_6H_9 intermediate, which further dehydrogenates to benzene between 290 and 340 K.[11,10,23,25,19] This dehydrogenation was shown to require an ensemble of ∼8 Pt atoms.[10] This adsorbed benzene intermediate, if present only at low coverage, further dehydrogenates to an intermediate of empirical formula C_2H at ∼540 K and finally to graphitic carbon between 550 and 800 K.[10,29,30]

Alkanes have not been studied previously with surface science techniques on Pt/ZnO model catalysts. However, the interaction of ethylene has been studied on 3 ML Pt films on ZnO(0001)−Zn with HREELS.[31] These films were highly stepped with many low coordination sites, allowing for stabilization of the π-bonded species to temperatures 200 K higher than on close-packed Pt(111), where the di-σ bonded species predominates above 40 K.[31] This π-bonded ethylene is considered to be the primary intermediate in ethylene hydrogenation.[32] The extent of ethylene dehydrogenation on Pd/Al_2O_3 model catalysts was shown to increase with particle size from 30 to 1000 atoms, whereas supported Rh and Ir did not dehydrogenate ethylene.[32] Infrared spectroscopy of Pt/Al_2O_3 catalysts showed that cyclohexane dehydrogenates to π-bonded benzene at 300 K, followed by benzene dehydrogenation and desorption between 500 and 650 K.[33]

The growth of Pt on ZnO(0001)−O has been studied previously with Auger electron spectroscopy (AES),[34] high-resolution electron energy loss spectroscopy (HREELS) and low energy electron diffraction (LEED),[35] and Li^+-ion scattering spectroscopy (LEIS).[36]

* To whom correspondence should be addressed.
† Current address: Department of Applied Physics, Chalmers University of Technology, S-412 96 Göteborg, Sweden.

10.1021/jp021907h CCC: $25.00
Published on Web 01/11/2003

2. Experimental Section

The experiments were performed in an ultrahigh vacuum (UHV) apparatus described previously[37−39] with a base pressure of less than 2×10^{-10} Torr. It has capabilities for XPS, LEED, LEIS, and TPD using a line-of-sight quadrupole mass spectrometer interfaced to a computer for multiplexing masses.

All XPS spectra reported here used Al Kα radiation (1486.6 eV). All LEIS spectra were taken using He^+ ions from an LK Technologies ion gun, with a primary ion energy of 700 eV, a scattering angle of 135°, and a He pressure of 4×10^{-7} Torr as read by the ion gauge (giving an ion current of ∼20 nA/cm^2). The detection angle was normal to the surface in both XPS and LEIS unless otherwise stated. The TPD experiments were done with a heating rate of ∼5 K/s.

The polished ZnO(000$\bar{1}$)-O crystal (Commercial Crystal Laboratories) was mounted on a small Ta back plate, such that tabs could fasten the crystal flush to the back plate. The temperature of the sample was varied through resistive heating and liquid-nitrogen cooling of this Ta backplate, allowing sample temperatures to vary between ∼140 and 1000 K. Sample temperatures were monitored with a thermocouple attached directly to the edge of the ZnO using a high-temperature UHV alumina-based ceramic adhesive (AREMCO).

Routine cleaning of the ZnO(000$\bar{1}$)−O sample consisted of sputter cleaning with 700 eV Ar^+ ions followed by annealing at 900−950 K for 20 min and a short 5 min anneal in 1×10^{-8} Torr O_2 followed by cooling in this O_2 atmosphere. This resulted in a good p(1 × 1) LEED pattern and clean surface as shown with LEIS and XPS. Platinum was vapor-deposited from a doser consisting of a high purity 0.1 mm diameter Pt wire coiled tightly around a 0.25 mm diameter W wire, which was resistively heated. This was mounted inside a stainless steel cover cap with an orifice for directed Pt flux. The Pt deposition rate was monitored by a water-cooled quartz crystal microbalance (QCM), an Inficon model XMT/2. The flux was corrected for the fact that the QCM could not be placed at exactly the same position as the sample using a scaling factor estimated from the geometry. The dose rates used varied between 0.1 and 0.25 ML/min. One Pt ML is defined as 1.505×10^{15} atom /cm^2, the packing density of the Pt(111) surface plane, corresponding to 0.225 nm thickness. This corresponds to ∼1.36 Pt atoms for each oyygen surface atom or ZnO(0001)−O unit cell. (This face of ZnO has 1.1×10^{15} O atoms/cm^2.)

The cyclohexane used was 99+% pure (Sigma-Aldrich) with water as the major impurity. The perdeuterated cyclohexane used contained 99.6 atom % D (Sigma-Aldrich). Both molecules were transferred to the dosing apparatus under an inert gas atmosphere and further purified with several freeze−pump−thaw cycles. The purity was verified with mass spectrometry. All cyclohexane exposures used a directed doser, as described previously.[38] Experiments to check the enhancement factor of the doser over backfilling the chamber with cyclohexane showed that the enhancement factor was ∼6. This was used in reporting exposures, but should only be considered accurate to within a factor of 2. In reporting exposures, the ion gauge reading was used directly without correction for the sensitivity factor of cyclohexane relative to N_2.

3. Results and Discussion

3.1. Pt Growth on ZnO(0001)−O. The growth of Pt on ZnO(0001)−O was studied with He^+ ion scattering spectroscopy (LEIS) at 300 K. We assume here that the Pt grows as islands, which is common for Pt growth on such oxides at 300 K.[40−43] Figure 1 shows the change in the integrated intensities of the Pt and Zn (substrate) LEIS peaks with increasing coverage of vapor-deposited Pt. The Pt flux was monitored with a quartz-crystal microbalance, and the coverage was further verified with XPS (see below). The normalized LEIS intensity is the integrated Pt LEIS intensity normalized to the maximum Pt LEIS integrated intensity when the surface is completely covered by a thick Pt film (Pt/Pt bulk). This normalized intensity provides a quantitative measure of the fraction of the surface covered by Pt islands, assuming that the He^+ neutralization probability is independent of metal island size, as is usually the case.[38,37]

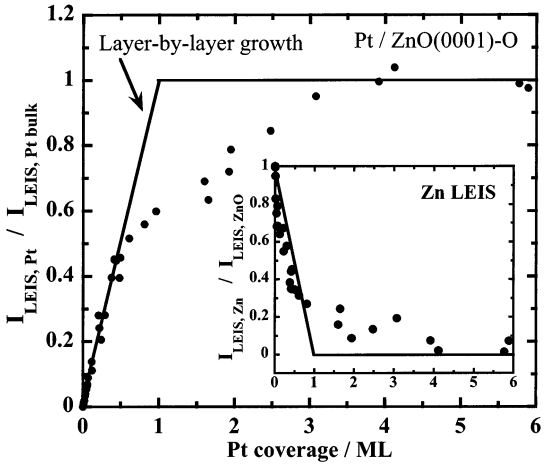

Figure 1. Pt LEIS intensity as a function of increasing Pt coverage on ZnO(0001)−O at 300 K. The Pt LEIS intensity has been normalized to a multilayer coverage of Pt where the Pt LEIS intensity has saturated (see text for details). The inset shows the normalized substrate Zn LEIS intensity as a function of increasing Pt coverage. It has been normalized to the Pt-free Zn LEIS intensity, which was ∼19% of the saturation Pt LEIS intensity. The solid lines in both cases show the behavior expected for layer-by-layer growth.

As seen in Figure 1, there is a linear increase in the normalized Pt LEIS signal up to ∼0.5 ML, indicating that the Pt islands are only one atom thick (i.e., 2D) up to this point. Above ∼0.5 ML, the signal shows an ∼6-fold decrease in slope. This implies a dramatic increase in the probability that an incoming Pt atom will diffuse to sites on the top of existing Pt islands rather than sites on the ZnO substrate. This transition has been called the "critical coverage" for the onset of bilayer or multilayer growth after a period of 2D island growth[40] and was observed for Cu on this surface.[37] Above this critical coverage, the Pt islands grow mainly thicker and their lateral spreading is slow but still faster than observed for Cu islands on this surface.[37] The sharp 2D/3D transition seen in this 2D island growth mode has been explained previously with a kinetic model.[37,40,44] However, it could also arise because of the strain in the substrate surface near small islands, which starts to overlap with strain because of other islands at coverages near 1/2 ML.[45,46] By ∼4 ML of Pt, the LEIS signal shows that the surface is completely covered by Pt.

The inset in Figure 1 shows the attenuation of the normalized Zn LEIS integrated intensity as a function of Pt coverage. The substrate signal is not attenuated by the incoming Pt atoms at the same rate that the Pt LEIS signal grows but is attenuated faster initially. This is probably because Pt adsorbs preferentially at defects[35,41,40,43] and the Zn-LEIS signal should be stronger at defects than on terrace sites (for example, because of the absence of surface oxygen atoms which mask the Zn atoms and/or a lower He^+ neutralization probability at defects). The Zn LEIS substrate signal was attenuated faster than the Pt signal grew also on the Zn-terminated ZnO(0001)−Zn surface,[47]

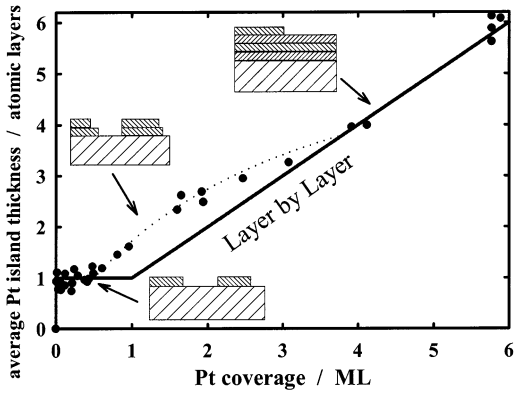

Figure 2. Average Pt island thickness in atomic layers as a function of increasing Pt coverage on ZnO(0001)−O at 300 K. This was calculated from the Pt LEIS data in Figure 1 whereby the Pt coverage in ML is divided by the fraction of the surface covered by Pt islands. (One atomic layer of Pt thickness is defined as the Pt(111) layer thickness, 0.225 nm.) The solid line is the expected behavior for layer-by-layer growth. The drawings are models of the surface structure.

consistent with this explanation. Zn was chosen to measure the substrate signal because it is both a stronger scatter (i.e., larger signal) than O and it avoids the possible complication of oxygen impurity signal from adsorbed CO or H_2O on the Pt.

The average Pt island thickness, t_{LEIS}, is merely the average thickness of deposited Pt divided by the fractional coverage by Pt islands determined by LEIS: $t_{LEIS} = d/\theta_{LEIS}$, where d is the deposited thickness and θ_{LEIS} is the fraction of the surface covered by Pt islands, equal to the normalized Pt LEIS signal. (Below, we refer to θ_{LEIS} as the "Pt area fraction".) The average island thickness is shown in Figure 2 versus Pt coverage. The dots are the actual data, and the solid line is the behavior expected for layer-by-layer growth. Up to 0.5 ML, the islands are one atomic layer thick and follow the layer-by-layer model. In this 2D island regime, the average island area probably increases roughly proportional to the Pt coverage above 0.1 ML, although we have no data that proves this. (This assumes that the number density of islands remains constant from 0.1 to 0.5 ML, which is typical of such metal-on-oxide systems.[48,49])

The integrated $Zn(2p_{3/2})$ and Pt(4f) XPS intensities normalized to the Pt-free $Zn(2p_{3/2})$ integrated intensity ($Zn(2p_{3/2})^o$) are shown in Figure 3 as a function of increasing Pt coverage at both normal (0°) and 60° detection angle. The solid lines correspond to the flat island model,[50] which assumes that the Pt islands are uniform in thickness and that island edge effects are negligible and uses the Pt area fraction (θ_{LEIS}) and average Pt island thickness as determined from LEIS (Figure 2). Because previous LEED and Li^+ LEIS data implied flat islands,[36,35] this is considered a good approximation. The XPS intensities of the substrate, I $Zn(2p_{3/2})$, and the adsorbate, I Pt(4f), normalized to that of the $Zn(2p_{3/2})^o$ peak from Pt-free ZnO, are given in this model by:

$$\frac{I\,\mathrm{Zn}(2p_{3/2})}{I\,\mathrm{Zn}(2p_{3/2})^o} = 1 - \theta_{LEIS} + \theta_{LEIS}\exp\left(\frac{-t_{LEIS}}{\lambda_{Zn,Pt}\cos\theta_d}\right)$$

$$\frac{I\,\mathrm{Pt}(4f)}{I\,\mathrm{Zn}(2p_{3/2})^o} = \frac{S'_{Pt}\lambda_{Pt,Pt}N_{Pt}}{S'_{Zn}\lambda_{Zn,Zn}N_{Zn}}\theta_{LEIS}\left(1 - \exp\left(-\frac{t_{LEIS}}{\lambda_{Pt,Pt}\cos\theta_d}\right)\right)$$

Here, θ_{LEIS} is the fractional coverage of the ZnO substrate by Pt islands as determined by Pt LEIS in Figure 1, t_{LEIS} is the average thickness of the islands, as shown in Figure 2, and θ_d is the detection angle of the analyzer relative to surface normal. The literature values used are as follows: surface sensitivity factors, S'_x, are 1.64 for $Pt(4f_{7/2})$ and 4 for $Zn(2p_{3/2})$;[51] inelastic mean free paths, $\lambda_{x,x}$, are 16.7 Å for Pt photoelectrons through Pt and 15.8 Å for Zn(2p3/2) photoelectrons through Zn;[52] and bulk atomic packing densities are 6.62×10^{22} Pt atoms/cm^3 for Pt and 4.15×10^{22} Zn atoms/cm^3 for ZnO.[53] These combine to give a literature value for the ratio of bulk XPS sensitivity factors of Pt(4f)/$Zn(2p_{3/2})$ of 0.65.

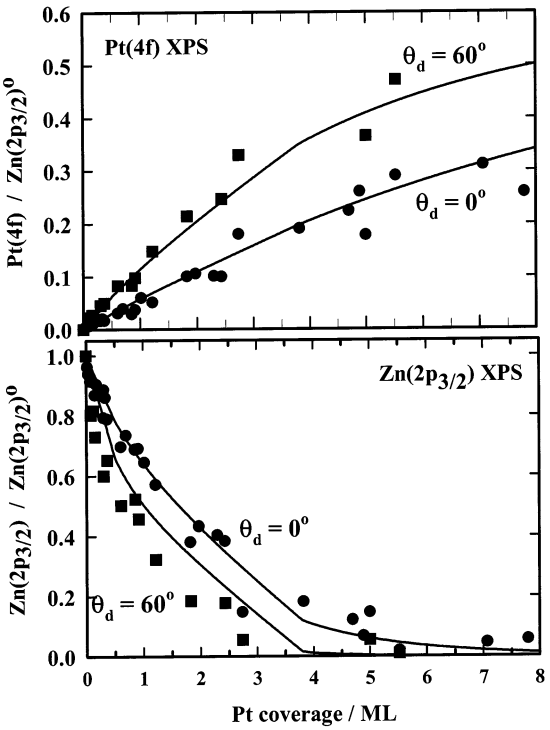

Figure 3. Variation in the Pt(4f) XPS integrated intensity and $Zn(2p_{3/2})$ XPS integrated intensity as a function of increasing Pt coverage at 300 K with both normal detection (circles) and 60° from normal (squares). The solid curves are fits of the data to a flat island model described in the text.

When fitting the substrate attenuation (bottom of Figure 3) to this flat island model, the inelastic mean free path of Zn photoelectrons through Pt, $\lambda_{Zn,Pt}$, was treated as the variable parameter. The best fit at 0° was obtained with a value of ~4 Å. This value does not fit so well at 60°, probably because of defocusing by Pt of a photoelectron diffraction peak at that angle (see below). However, using the standard layer-by-layer growth model[54]

$$\frac{I\,\mathrm{Zn}(2p_{3/2})}{I\,\mathrm{Zn}(2p_{3/2})^o} = \exp\left(-\frac{t_{Pt,ML}}{\lambda_{Zn,Pt}\cos\theta_d}\right)$$

where $t_{Pt,\,ML}$ is the thickness of the deposited Pt in Å, the best fit value of $\lambda_{Zn,Pt}$ using both detection angles was 4.5 Å. The similarity in this best-fit parameter in these two different structural models emphasizes the need to use an elemental analysis technique with a shallower probe depth than XPS or AES to determine the growth modes of such systems. The LEIS data of Figure 1 provide that greater surface specificity here.

The best fit value of $\lambda_{Zn,Pt}$ mentioned above is 4.0 Å, much shorter than the literature value of 7.8 Å.[52] We also studied the growth of Pt on ZnO(0001)−Zn surface, where the attenuation of the Zn signal gave $\lambda_{Zn,Pt}$ of 5.2 Å,[47] again shorter. This suggests that the literature value may be too long. Contributing also to this difference may be the fact that the Zn(2p)

photoelectrons are strongly forward focused at 0° and near 60° because of diffraction effects from this ZnO(0001)−O face.[37] These photoelectrons might be scattered out of the acceptance cone of the analyzer by the Pt atoms of the deposited overlayer (depending on their locations relative to the substrate atoms), leading to a smaller $\lambda_{Zn,Pt}$ than expected from literature values and a uniform overlayer density model.[55]

The adsorbate Pt(4f) XPS intensities were also fit with the flat island growth model, as shown in the top panel of Figure 3, treating the ratio of bulk XPS sensitivity factors, Pt(4f):Zn-($2p_{3/2}$), and $\lambda_{Pt,Pt}$, as fitting parameters. As described above, the ratio of bulk sensitivity factors calculated using literature values is 0.65, just 10% less than the resulting best-fit value (0.59). The best-fit value for $\lambda_{Pt,Pt}$ was 21 Å, about 30% larger than the literature value (16.7 Å[52]), but within its possible error.

It has been previously reported that Pt grows in a nearly layer by layer fashion on ZnO(0001)−O.[36,35,34] However, the subtle difference between the actual growth mode reported here (Figures 1 and 2), and a layer-by-layer mode could probably not have been detected in those studies, because they relied on elemental analysis techniques with much deeper probe depths than the He^+ LEIS used here[34,35] or had a less well-defined coverage calibration.[36] Nevertheless, those earlier studies[36,35,34] provide important complimentary information on the structure of the Pt films and particles.

Using Li^+ LEIS, Radulovic and Overbury found some indication that Pt islands form and are thicker at a given Pt coverage on the O-terminated face than on the Zn-terminated face, with less azimuthal alignment with the substrate.[36] This is consistent with our finding of a slightly lower critical coverage than that seen on the Zn-terminated face (0.7 ML[47]), leading to thicker islands on the O-terminated face. Curiously, the growth of Cu on these two faces of ZnO showed a slightly higher critical coverage on the O face than on the Zn face,[38,37] the reverse of that seen here. This may be related to differences in the density of defects that nucleate clusters.

3.2. Thermal Sintering of Pt Particles on ZnO(0001)−O. The thermal sintering of these Pt particles was studied using Temperature Programmed LEIS (TP-LEIS), which consisted of continuously monitoring the normalized Pt LEIS peak height (fractional coverage by Pt islands) during a linear temperature ramp (~1 K/s) to 850 K after Pt deposition at 300 K. These experiments, shown in Figure 4, revealed a distinctly more facile sintering of the Pt islands on this O-terminated face of ZnO, compared to our previous results for the Zn-terminated face.[47] Briefly, after depositing a large coverage of Pt (~3 ML) at 300 K and then ramping the temperature, the Pt islands on this O face sintered starting at ~600 K until they cover only 40% of the surface by 800 K, compared to ~65% on the Zn-face. More interestingly, when starting with Pt coverages below 0.5 ML, where the islands are still 2D, heating to 800 K results in thicker particles which cover ~40−60% less of the surface after annealing to 800 K. The TP-LEIS data indicates that the 2D islands start to thicken and sinter at ~600 K. No thickening of 2D Pt islands was observed on the Zn face, even up to 800 K.[47] This difference between these two polar ZnO faces was not seen by either Gorte or Petrie using less surface sensitive techniques[35,34] but was seen by Radulovic et al. using Li^+LEIS.[36]

The more facile sintering of 2D Pt islands on the O-face suggests that the upstepping barrier for a Pt adatom at the edge of a 2D island is smaller on the O-term face than on the Zn-terminated face, as postulated previously.[36] This would suggest that Pt in 2D islands is more weakly bound to the O-face of ZnO than to the Zn face. This is consistent with the lower critical coverage seen on the O-terminated face. Parker et al.[44] showed that the critical coverage decreases as the diffusion constant for the metal adatom on the substrate increases, which is expected if the bonding is weaker.

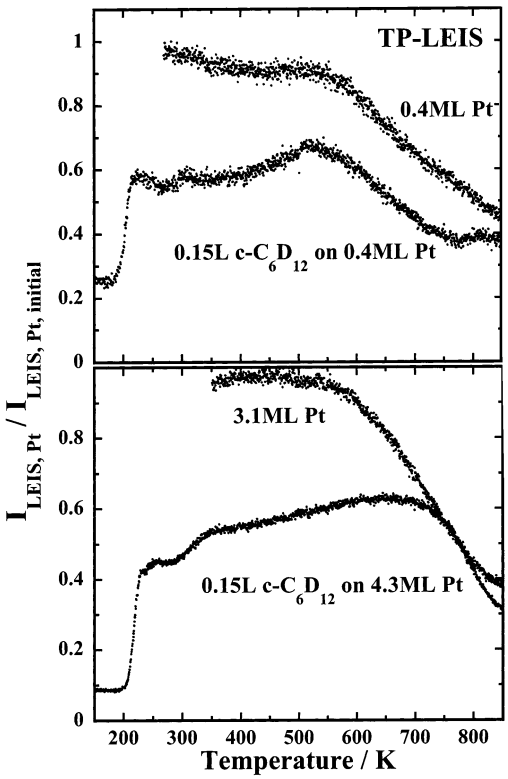

Figure 4. Pt LEIS signal (relative to its initial value before dosing *c*-C_6D_{12} or heating) monitored continuously during heating of Pt particles on ZnO(0001)−O, with and without a 0.15 L postdose of *c*-C_6D_{12} at ~170 K. Results are shown for 2D islands of Pt (~0.4 ML Pt) and a thick Pt film (~4 ML Pt). Heating rate = 1 K/s.

3.3. H_2 Adsorption on ZnO(0001)−O and 2D and 3D Pt Islands on ZnO(0001)−O. No evidence was seen in TPD for hydrogen adsorption on Pt-free ZnO(0001)−O after dosing ~2 L of H_2 at 200 K. When ~2 L of H_2 is dosed to these supported Pt particles on ZnO(0001)−O at ~200 K, a broad H_2 peak appears at ~330 K in subsequent TPD, as shown in Figure 5. The H_2 desorption temperature at all Pt coverages is quite similar to that seen on Pt(111)[56,57] and other bulk Pt faces.[58] The area of this TPD peak increases nearly linearly with the Pt island area fraction (θ_{LEIS}), as seen in Figure 6. These experiments were performed by dosing Pt to clean ZnO at 300 K, cooling off the sample to ~200 K, flashing to ~600 K to desorb any background gases, and rapidly recooling to ~200 K. Next, the resulting surface was exposed to ~2 L of H_2, and TPD was run immediately. Subsequent Pt coverages were deposited on top of the previously deposited Pt islands, and the same H_2 dosing procedure outlined above was used. Note that the Pt fractional coverages in Figure 4 were measured by LEIS before the sample was flashed to 600 K. The actual fractional coverages after this flash are slightly lower because of the onset of sintering at ~600 K (see above).

A 7 L dose of D_2 at ~200 K to a Pt precoverage of 0.7 ML caused the Pt LEIS signal from these Pt islands to decrease by ~50%. A 1.2 L dose of D_2 to a Pt precoverage of 5 ML caused the Pt LEIS signal to decrease by ~35%. Thus, D(a) or H(a) on these Pt islands attenuates the Pt LEIS signal substantially.

3.4. Cyclohexane Adsorption on Pt-Free ZnO(0001)−O. To our knowledge, this is the first study of the adsorption of a

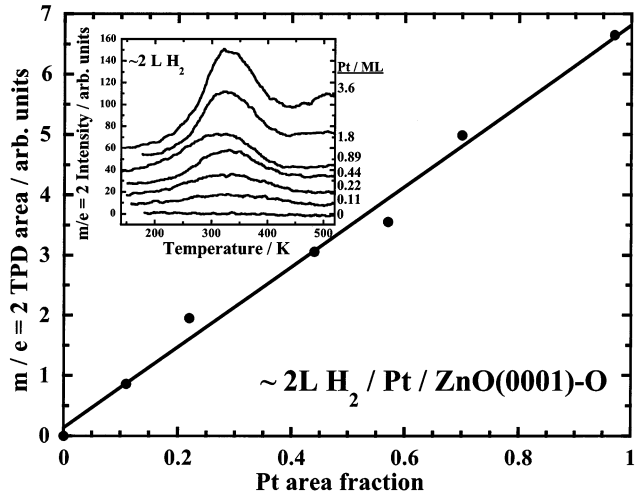

Figure 5. Variation in the integrated H_2 TPD area after dosing ~2 L of H_2 to increasing coverages of vapor-deposited Pt on ZnO(0001)−O at ~200 K. The *x* axis plots this Pt coverage as the Pt area fraction (i.e., the fraction of the ZnO surface covered by Pt islands as measured by LEIS (Figure 1)). The inset shows the TPD spectra for various Pt precoverages. This sample has been treated differently before these TPDs than in subsequent figures, in a way which tends to saturate the near bulk of the ZnO with H and inhibit its loss to the bulk in TPD relative to subsequent figures (see text). Note also that H is expected to diffuse less readily in to the bulk than D (see below). The lower peak temperature at 0.89 ML is due to the lower dose temperature (~150 K) used, as is also seen on Pt(111).

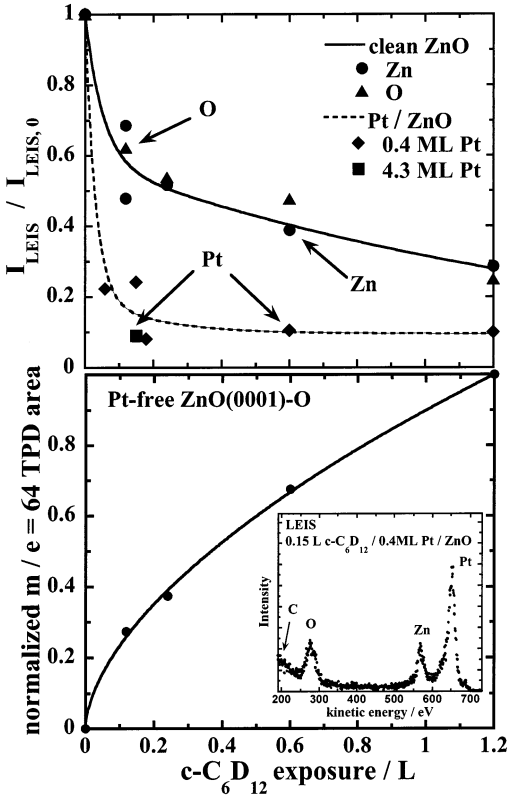

Figure 6. Top: (a) Attenuation of the integrated Zn and O LEIS intensities from the Pt-free ZnO(0001)−O surface with increasing *c*-C_6D_{12} exposure at 170 K. The exposures are in langmuirs (1 L = 10^{-6} Torr s, corrected for the enhancement factor of the doser. (b) The attenuation of the integrated Pt LEIS intensity of a ZnO(0001)−O surface predosed with 0.4 ML Pt with increasing *c*-C_6D_{12} exposure at 170 K. Bottom: The corresponding TPD peak areas for molecular *c*-C_6D_{12} desorption from Pt-free ZnO versus *c*-C_6D_{12} exposure at 170 K (see Figure 7). Inset: A typical LEIS spectrum of a Pt/ZnO(0001)−O surface dosed with 0.15 L *c*-C_6D_{12} at 170 K.

cyclic alkane on ZnO(0001)−O. Figure 6 shows the attenuation of the normalized Zn LEIS peak intensity with increasing exposure of cyclohexane to Pt-free ZnO(0001)−O at ~160 K. All exposures reported here have been corrected for the enhancement factor of the directed doser (~6). The substrate signal was ~85% attenuated by an exposure of 3.6 L (1 L = 10^{-6} Torr s), suggesting that a nearly close-packed monolayer is formed. (This adsorption temperature was too warm to populate the multilayer TPD peak.) A similar attenuation of the O-LEIS peak was seen (Figure 6), along with a corresponding growth in LEIS intensity below 240 eV, attributed to carbon LEIS signal.

The saturation cyclohexane coverage gave a C(1s)/Zn($2p_{3/2}$)^o XPS intensity ratio of 0.0048. (The superscript "o" here refers to the Pt-free ZnO surface.) In a quantitative XPS study of cyclohexane adsorption on Pt(111), a saturated monolayer (1.0 ML) of cyclohexane (3.2×10^{14} cyclohexanes/cm^2) gave a C(1s)/Pt($4f_{7/2}$) XPS ratio of 0.0172.[10] Utilizing this value and the ratio $[S'_{Pt}\lambda_{Pt,Pt}N_{Pt}]/(S'_{Zn}\lambda_{Zn,Zn}N_{Zn}]$ of 0.59 determined above and correcting for the known sensitivity ratio for Pt(4f):Pt($4f_{7/2}$) of 7:4,[51] we can predict a C(1s)/Zn(2p3/2)^o XPS ratio of $0.0172 \times 0.59 \times 4/7 = 0.0058$ if we had this same cyclohexane packing density on ZnO(0001)−O. This is close to the experimental value seen here, and indicates that the monolayer cyclohexane packing density on ZnO(0001)−O surface is quite similar to that on the Pt(111) surface. This is not surprising because it corresponds to nearly close-packing of cyclohexanes on Pt(111).[10,59] The intensity of the C-LEIS signal on this Pt-free surface after ~3.6 L of cyclohexane is about the same as seen on a surface precovered by ~10 ML of Pt after ~3.6 L of cyclohexane, also suggesting similar packing densities on Pt and ZnO.

When the ZnO surface dosed with cyclohexane at 170 K was heated to ~300 K, the Zn-LEIS peak intensity was restored, the C-LEIS peak was removed, and the C(1s) XPS peak returned

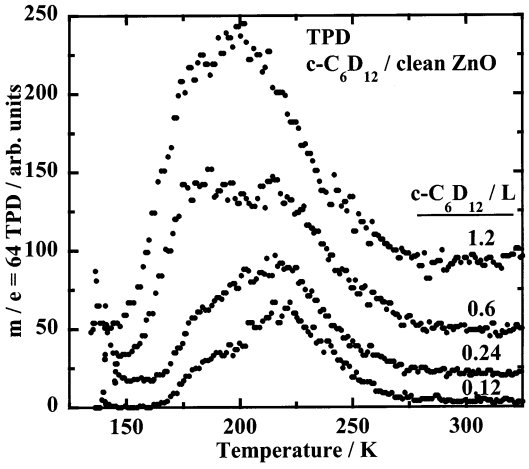

Figure 7. TPD of molecular *c*-C_6D_{12} from ZnO(0001)−O for increasing exposure of *c*-C_6D_{12} at 160 K.

to baseline. The intact molecular desorption of *c*-C_6D_{12} was seen in a TPD peak at ~210 K (see Figure 7). Assuming a typical prefactor for desorption of 10^{13} s^{-1}, this corresponds to an activation energy for desorption (~the heat of adsorption) of ~52 kJ/mol.[60] Complicating the TPD spectra was a broad TPD peak with the same cracking pattern as cyclohexane seen between 300 and 600 K. This peak does not saturate with

TABLE 1: Peak Temperatures in TPD after Exposure of Cyclohexane or Benzene onto Low Index Pt Single Crystal Surfaces[a]

surface	molecule dosed	molecular desorption	H_2 (or D_2) dehydrogenation product	ref
Pt(111)	c-C_6H_{12}	154, 181, and 236 K	365,[b] 540, and broad 680 K	10
Pt(100)−(1 × 1)	c-C_6H_{12}	n/a	350, 450, 540,[b] and broad 680 K	16
Pt(100)−(5 × 20) or hex	c-C_6H_{12}	n/a	very small 450 K	16
Pt(111)	c-C_6H_6	195, 350, and 505 K	540[b] and broad 650 K	29
Pt(111)	c-C_6D_6	370−490 K	∼560[b] and broad 650K	29,28,63
Pt(111)-steps	c-C_6D_6	450−480 K	∼470 and broad 630 K	29,28,63
Pt(100)−(1 × 1)	c-C_6H_6	n/a	450, 540,[b] and broad 680 K	16
Pt(110)−(1 × 2)	c-C_6D_6	185, 280, and 400 K (only > 0.15 ML)	450, 545,[b] and broad 640 K	62,30
Pt(100)−(5 × 20) or hex	c-C_6H_6	n/a	broad 450 and broad 680 K	16

[a] Note: "n/a" indicates that this value was not determined in reference(s) cited. [b] The most intense peak.

increasing cyclohexane exposure, is not dependent on the presence of Pt on the sample, and is not accompanied with LEIS intensity changes expected for desorption of cyclohexane from the surface. It cannot be produced when both the sample holder and sample are at 300 K during dosing but is produced if the sample is held at 300 K with the sample holder at 150 K during dosing. These controls prove that this broad peak is not from ZnO but instead arises from desorption of physisorbed cyclohexane on some part of the sample holder which warms slightly during sample heating. It will not be discussed further below.

With a properly prepared ZnO(0001)−O surface, no H_2 or D_2 was seen desorbing in TPD following exposures to c-C_6H_{12} or c-C_6D_{12}, respectively. However, if the ZnO sample was only annealed in UHV after sputter cleaning (for example, to remove Pt and C from a previous experiment), without annealing in O_2, then a high-temperature (∼750 K) peak was seen for H_2 (or D_2) in TPD which persisted to the highest temperature studied (800 K) and which contained important contributions from the other isotope if used in recent sample history. Similar results were seen with benzene[61] and attributed to the dissociative adsorption of the hydrocarbon on defect sites (possibly oxygen vacancies) on this ZnO surface which are removed by annealing in oxygen. The high temperature of the peak and its isotopic memory suggest that the hydrocarbon deposits H (or D) into the near-surface bulk of the ZnO, from whence it returns to the surface at ∼750 K and desorbs.

3.5. Review of Cyclohexane Adsorption and Dehydrogenation on Pt Single Crystals. The adsorption and dehydrogenation of cyclohexane has been studied extensively on a variety of Pt single-crystal surfaces,[9−28] and we summarize those results here and in Table 1 to make it easier to explain the results on Pt/ZnO below. Cyclohexane adsorbs molecularly at 100 K. On Pt(111), it desorbs at ∼230−240 K, in competition with dehydrogenation through the following steps:

$$c\text{-}C_6H_{12}(a) \rightarrow c\text{-}C_6H_9(a) + 3H(a) \text{ between } 230-300 \text{ K}$$
$$\rightarrow c\text{-}C_6H_6(a) + 6\,H(a) \text{ at } \sim 290-340 \text{ K} \quad (1)$$

$$2H(a) \rightarrow H_2(g) \qquad \text{at } \sim 350 \text{ K} \quad (2)$$

Given that the H desorbs as H_2 at ∼350 K from Pt(111), this H_2 peak is desorption rate limited. The formation of benzene begins at ∼290 K. On other faces, benzene is also produced and other intermediates have been suggested, such as 1,6-hexadialkylidene, cyclohexene, and cyclohexadiene. The dehydrogenation of cyclohexane is self-poisoned by high coverages of cyclohexane (and its decomposition products), as evidenced by a decreasing probability to dehydrogenate with increasing coverage.

The further dehydrogenation of the benzene begins at ∼450−540 K, and on Pt(111) occurs through a series of dehydrogenation steps:[29,30]

$$c\text{-}C_6H_6(a) \rightarrow 3C_2H(a) + 3H(a) \text{ at } \sim 540 \text{ K} \quad (3)$$

$$3C_2H(a) \rightarrow 6C(a) + 3H(a) \text{ between } 570-800 \text{ K} \quad (4)$$

The H(a) products of these benzene decomposition reactions desorb immediately as $H_2(g)$, giving rise to several H_2 TPD peaks. The H_2 peak at 540 K appears as D_2 at ∼20 K higher temperature when using perdeuterated cyclohexane (or benzene), because of the primary kinetic isotope effect on C−H vs C−D cleavage in the adsorbed benzene.[29] An H_2 TPD peak is seen at ∼400−470 K from benzene dehydrogenation on Pt(110)−(1 × 2) and at steps on Pt(111).[28,29,30,62,63] Upon complete dehydrogenation at ∼800 K, graphitic C(a) is left on the Pt surfaces.[29,30]

3.6. Cyclohexane Adsorption and Dissociation on 2D and 3D Pt Islands on ZnO(0001)−O. The adsorption and dehydrogenation of perdeuterocyclohexane (c-C_6D_{12}) was studied as a detailed function of Pt coverage on ZnO(0001)−O. Perdeuterated cyclohexane was used in the figures presented below to minimize complication from background H_2, but qualitatively similar results were observed also with nondeuterated cyclohexane. Although normal cyclohexane readily dehydrogenates on Pt(111), perdeuterocyclohexane was found to dehydrogenate on Pt(111) with only very low probability (<0.05) because of a primary kinetic isotope effect which decelerates C−D cleavage so much that molecular desorption instead dominates.[10] We show below that perdeuterocyclohexane readily dissociates on Pt particles on ZnO(0001)−O, which implies that this surface provides sites where the activation barrier for C−D cleavage is reduced or where the desorption rate is suppressed (because of a higher adsorption energy) or both.

Dosing cyclohexane to the surface containing preadsorbed Pt at ∼170 K attenuates the normalized Pt LEIS peak faster than the Zn peak of Pt-free ZnO, both for the cases of 2D Pt islands and a continuous multilayer Pt film, as shown in Figure 6. This indicates that c-C_6D_{12} adsorbs faster (i.e., with a higher sticking probability) on the Pt particles than on clean ZnO-(0001)−O. Oxide-supported metal particles often show very high adsorption rates because of gas molecules which strike the nearby oxide support and physisorb and then diffuse across the support surface to a metal particle and stick there.[42,64] If this capture-zone model were operative here, the attenuation of the Pt LEIS signal with hydrocarbon exposure would be faster for Pt islands at low Pt coverage than for a continuous, multilayer Pt film. However, the Pt LEIS signal for Pt islands decreased with hydrocarbon exposure (Figure 6) only as fast as it did for a continuous Pt film, at least within the scatter in

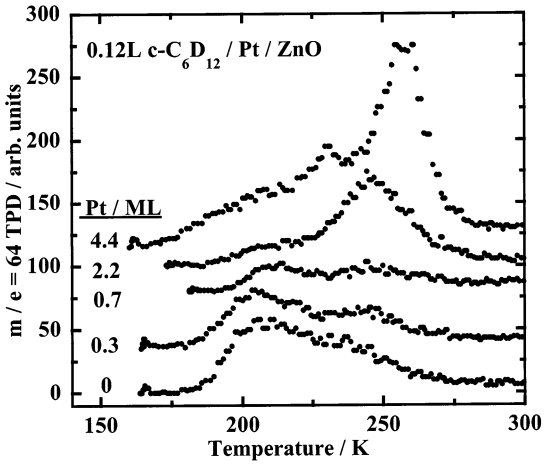

Figure 8. Typical TPD spectra showing molecular desorption of cyclohexane on Pt/ZnO(0001)−O after ∼0.12 L of *c*-C_6D_{12} was dosed at ∼170 K for several Pt coverages.

the data. At lower exposures than studied here, one might find evidence for this effect.

The C LEIS signal grows to approximately the same size at saturation on Pt-free ZnO and ZnO containing ∼4 ML of Pt. This indicates that the saturation coverage of *c*-C_6D_{12} on multilayer Pt is similar to that on Pt-free ZnO, consistent with the XPS results above which indicated similar saturation coverages on Pt(111) and ZnO(0001)−O. The similar relative attenuation of the Pt LEIS signal at saturation on the Pt islands (Figure 6) suggests that the local *c*-C_6D_{12} coverage on Pt islands is similar as well.

A series of TPD experiments to probe cyclohexane desorption and dehydrogenation was performed as follows. First, Pt was vapor-deposited onto clean ZnO(0001)−O at ∼300 K. Then the sample was cooled to ∼180 K, and XPS was taken while cooling to confirm the Pt coverage. Next, the sample was briefly flashed to ∼600 K to desorb any background gases such as H_2 and CO and quickly recooled. Then, ∼0.12 L of *c*-C_6D_{12} was dosed at a sample temperature of ∼170 K. According to LEIS and TPD (Figure 6), this exposure produces ∼40% of a monolayer (0.4 ML) of cyclohexane on clean ZnO(0001)−O but a higher coverage on the Pt particles (∼0.8 ML). A TPD was taken immediately after pump down (i.e., as soon as the mass spectrometer showed that the cyclohexane pressure was insignificant). Before another experiment, the surface was sputtered (to remove C and Pt), annealed in oxygen to order the ZnO, and finally dosed with fresh Pt. The TPD results are presented in Figures 8 and 9.

Molecular desorption of *c*-C_6D_{12} as a function of Pt precoverage is shown in Figure 8, the TPD spectra for $m/e = 64$, the most intense fragment in our mass spectrometer's cracking pattern of *c*-C_6D_{12}. On the Pt free surface, cyclohexane desorbs in a broad peak centered at ∼220 K. On thick Pt films, the cyclohexane desorbs in a peak centered at ∼250 K, similar to Pt(111). Thus, the integrated TPD area from ∼240 to 300 K for this mass can be attributed to cyclohexane desorption from Pt sites. This area is very small for Pt coverages below ∼0.5 ML and mainly attributable to contributions to the molecular desorption intensity from ZnO sites which extends slightly above 240 K. The 240−300 K intensity rapidly increases above 0.6 ML Pt, which we attribute to the expected increase in cyclohexane amount on Pt sites as the area of the Pt nanoparticles increases, compounded by a decrease in its dissociation probability with Pt nanoparticle thickness (which is near unity below 0.5 ML Pt, when the Pt islands are 2D).

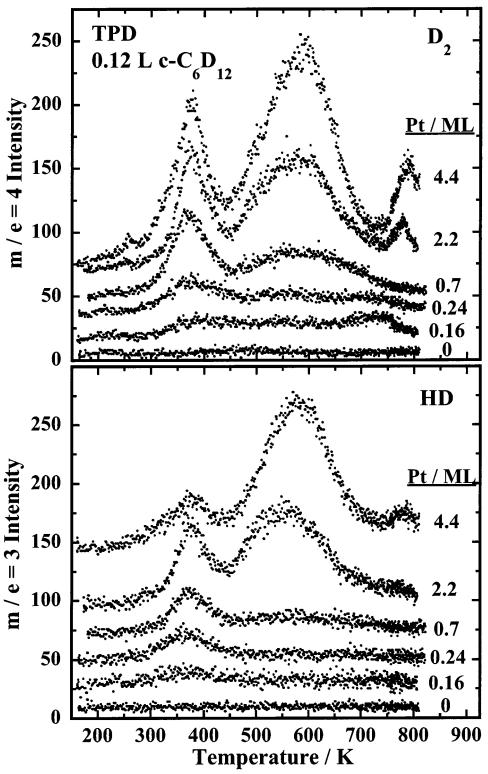

Figure 9. TPD spectra from the same data as Figure 8 showing the evolution of D_2 (top panel) and HD (bottom panel) after ∼0.12 L of *c*-C_6D_{12} at ∼170 K onto Pt/ZnO(0001)−O. The Pt was pre-deposited on the clean ZnO surface at 300 K and preflashed to ∼600 K before cyclohexane exposure.

Figure 9 shows the TPD of the dehydrogenation products, D_2 ($m/e = 4$) and HD ($m/e = 3$), after dosing *c*-C_6D_{12} to ZnO-(0001)−O with increasing Pt precoverages. (The amount of desorbing H_2 was very small and so not discussed further here.) On the Pt-free surface (bottom spectra), no significant desorption of D_2, HD, nor H_2 was seen. However, with Pt present, D_2 and HD both desorbed in a peak at ∼370 K and a broad peak at ∼580 K which extends from ∼450 to ∼750 K. On these Pt nanoparticles, the 370 K peak is assigned to dehydrogenation of cyclohexane to benzene, as also seen on Pt(111) (Table 1). The 450−750 K peak is attributed to a mixture of the 450, 540, and 570−750 K TPD peaks seen from *c*-C_6H_6 and *c*-C_6H_{12} dehydrogenation on different Pt single-crystal surfaces (see Table 1), corrected for the +20 K peak shift for D_2 versus H_2 because of the kinetic isotope effect mentioned above. We saw a very similar (but more intense) TPD peak after dosing benzene to Pt nanoparticles on ZnO(0001)−O, and it grew similarly with Pt coverage.[61] For this reason, we attribute this peak mainly to the dehydrogenation of adsorbed benzene, produced by cyclohexane dehydrogenation on the Pt particles below 400 K, just as it occurs on Pt single crystals. There is also a small peak at ∼780 K, which we attribute to D penetration into and subsequent removal from the near surface bulk of the ZnO crystal, based on prior reports of such a peak on ZnO[47,65−67] (see also below).

As the Pt coverage increases, all of these peaks increase in size to saturation. The total amount of dehydrogenation of *c*-C_6D_{12}, estimated from the total integrated areas of all D_2 peaks plus half the areas of the HD peaks, is plotted versus Pt area fraction in Figure 10. This increases slightly faster than linearly with Pt island area. We believe that this is because the adsorbed D produced on the 2D Pt islands (i.e., below 0.5 ML) has a

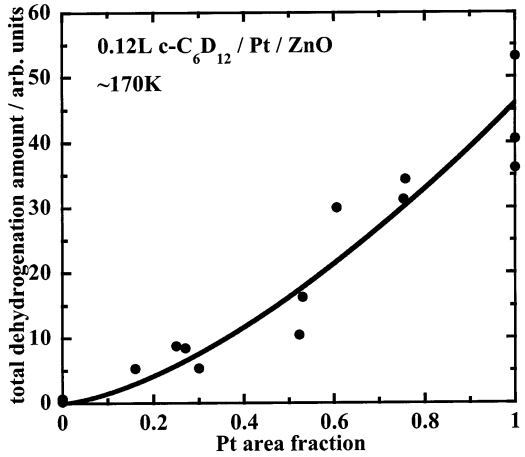

Figure 10. Variation with Pt area fraction in the total amount of dehydrogenation products for a dose of 0.12 L *c*-C_6D_{12}, measured by the integrated area of the $m/e = 4$ (D_2) TPD peaks plus half that for the $m/e = 3$ (HD) peaks, taken from more extensive data like those in Figure 9. The Pt area fraction here was measured by the Pt LEIS signal relative to that for a continuous multilayer Pt film (Figure 1). The line is meant to guide the eye.

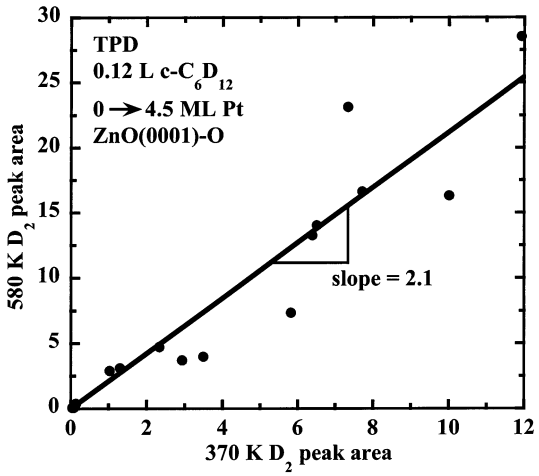

Figure 11. Area of the broad ~580 K D_2 peak (integrated from ~440 to 800 K) for a 0.12 L dose of *c*-C_6D_{12} at many Pt coverages (just as in the data of Figures 7−9), plotted versus the corresponding area of the ~370 K D_2 peak. The best-fit line shown has a slope ~2.1, rather than 1.0 expected for the benzene intermediate.

higher probability to be lost into the bulk during TPD than for thicker Pt particles (see below).

Figure 11 shows the areas of the broad ~580 K D_2 peak (integrated from ~440 to 800 K) for many Pt coverages plotted versus the corresponding area of the ~370 K D_2 peak. There is a nearly proportional relationship, with slope ~2.1. For cyclohexane on Pt(111), these peak regions have equal integrated intensities (slope ~1.0) because of the 1:1 stoichiometry: the first 6 H atoms are lost in dehydrogenation to benzene (below 400 K) and the last 6 are lost in benzene's dehydrogenation to graphitic carbon (above 450 K).[10] We believe the same stoichiometry pertains here, but that the lower temperature peak appears smaller than it should because it loses more D into the bulk of ZnO, causing its area to be smaller than predicted by stoichiometry alone.

Notice that the amount of HD seen in Figure 9 is nearly as large as the amount of D_2 and much, much larger than the amount expected based on the isotopic purity of the *c*-C_6D_{12} used (99.6 at. % D). However, there is much less HD seen in the 360 K peak relative to the 580 K peak, particularly at the Pt coverages above ~2 ML. This is attributed to isotopic scrambling of surface D with the subsurface H present in the near bulk of the ZnO crystal, which occurs more readily at higher temperature. (The near bulk contained H isotope because of previous experiments with H_2 and c−C_6H_{12}.) This is consistent with influences of the near-surface bulk ZnO also observed during TPD studies of methanol and formic acid dehydrogenation on supported Pt and Cu particles on ZnO-(0001)−Zn and ZnO(0001)−O, including: (1) loss of surface H and D into the ZnO bulk, (2) a greater extent of such loss with lower-temperature H_2 (or D_2) TPD peaks and at lower metal coverage, (3) H/D isotopic scrambling with the bulk H/D pool for ~500−700 K H_2 (or D_2) TPD peaks, and (4) near-surface bulk H (or D) desorption as H_2 (or HD or D_2) at 750−800 K.[47,65−67] A kinetic effect was also reported which favors the loss into the bulk of surface D over H.[65] The contribution from HD in the ~360 K peak was consistently very small relative to that from D_2 for Pt coverages of ~3 ML and above (Figure 9). This suggests that isotopic scrambling between surface-bound D and near-bulk H at 360 K is nearly suppressed for such a thick and continuous Pt film.

We did not detect any molecular benzene desorbing from the benzene product which we propose is formed on these supported Pt particles during heating of adsorbed cyclohexane. This is consistent with studies on low index Pt single-crystal surfaces which have shown that, at low to moderate benzene coverages, all of the benzene decomposes during TPD.[29,30,62]

Before the above TPD studies with *c*-C_6D_{12}, we performed similar TPD studies with unlabeled cyclohexane (*c*-C_6H_{12}). Qualitatively similar behavior to Figures 8 and 9 was observed but with H_2 as the only dehydrogenation product.

Figure 4 shows the Pt LEIS signal monitored continuously during heating of 2D (0.4 ML) and 3D (4 ML) Pt particles on ZnO(0001)−O, with and without a 0.15 L postdose of *c*-C_6D_{12} at ~170 K. Without *c*-C_6D_{12}, the signal remains stable up to ~600 K, above which it starts to decrease becaus of sintering of the Pt into larger, thicker particles which cover a smaller fraction of the ZnO surface as described above. With the 0.15 L dose of *c*-C_6D_{12}, there is a ~80−90% decrease in the Pt LEIS signal, corresponding to 0.8−0.9 ML of adsorbed *c*-C_6D_{12}. About 40% of this decrease is recovered at ~ 220 K in TP-LEIS, because of either the molecular desorption of adsorbed *c*-C_6D_{12} or the first step in its dehydrogenation, which occurs at about this temperature on Pt surfaces[11,25,19] and could decrease the He^+ neutralization probability. Even if all of this increase in Pt LEIS signal at 220 K is due to molecular desorption, it gives a maximum desorption probability of ~0.4 and, thus, a probability for dehydrogenation of at least 0.6, almost independent of Pt coverage. Independence of dehydrogenation probability on Pt coverage at this high cyclohexane coverage could occur because of self-poisoning of Pt sites by its decomposition products, which could limit the extent of dehydrogenation to a maximum packing density, independent of how reactive the surface is in abstracting D from the molecule. From 250 to 650 K, the Pt LEIS signal remains below that for cyclohexane-free Pt/ZnO, because of masking of the Pt signal by these adsorbed products of dehydrogenation. Above 700 K, the Pt LEIS signal approaches that seen with no cyclohexane dose, suggesting that these products desorb (as D_2 and DH) and convert to a product that masks little of the surface. On Pt(111), the C product of benzene dehydrogenation rearranges at this temperature into graphitic C,[29] which covers only a small fraction of the surface.[68]

4. Conclusions

These results show that supported Pt particles are much more active in dehydrogenating perdeuterocyclohexane relative to bulk Pt(111), which shows <0.05 probability for dehydrogenation of c-C_6D_{12} during TPD even at low coverages.[10] The very weak molecular desorption signal for Pt coverages of 0.3 and 0.7 ML in Figure 8, where the Pt islands are only ~1 atom thick but cover 30−60% of the surface, suggests that the dehydrogenation probability of c-C_6D_{12} on 2D Pt islands is near 100% for this small c-C_6D_{12} exposure (0.12 L or ~0.8 ML on the Pt particles). The increase in the molecular desorption signal for larger Pt coverages (thicker particles) suggests that the dehydrogenation probability depends on particle size, with the thinnest (smallest) particles being most active, thicker particles and rough films being less active, and large Pt(111) facets being least active.

Acknowledgment. The authors would like to acknowledge the Department of Energy, Office of Basic Energy Sciences, Chemical Sciences Division, for support of this work. L.T.N. would like to thank the University of Washington Center for Nanotechnology for an NSF-IGERT graduate research fellowship.

References and Notes

(1) Sinfelt, J. H. *J. Mol. Catal. A*: *Chem.* **2000**, *163*, 123−128.
(2) Alexander, B. D.; Huff, G. A. J. *Dehydrogenation Catalyst and Process*; Amoco Corporation: US, 1995.
(3) Ohta, M.; Ikeda, Y.; Igarashi, A. *J. Jpn. Pet. Inst.* **2002**, *45*, 144−149.
(4) Claus, P. *Top. Catal.* **1998**, *5*, 51−62.
(5) Consonni, M.; Jokic, D.; Murzin, D. Y.; Touroude, R. *J. Catal.* **1999**, *188*, 165−175.
(6) Cubeiro, M. L.; Fierro, J. L. G. *J. Catal.* **1998**, *179*, 150−162.
(7) Takezawa, N.; Iwasa, N. *Catal. Today* **1997**, *36*, 45−56.
(8) Iwasa, N.; Akazawa, T.; Ohyama, S.; Fujikawa, K.; Takezawa, N. *React. Kinet. Catal. Lett.* **1995**, *55*, 245−250.
(9) Blakely, D. W.; Somorjai, G. A. *J. Catal.* **1976**, *42*, 181−196.
(10) Rodriguez, J. A.; Campbell, C. T. *J. Phys. Chem.* **1989**, *93*, 826−835.
(11) Bussell, M. E.; Henn, F. C.; Campbell, C. T. *J. Phys. Chem.* **1992**, *96*, 5978−5982.
(12) Campbell, C. T.; Rodriguez, J. A.; Henn, F. C.; Campbell, J. M.; Seimanides, S. G. *J. Chem. Phys.* **1988**, *88*, 6585−6593.
(13) Campbell, C. T. *Crit. Rev. Surf. Chem.* **1994**, *3*, 49−75.
(14) Newton, M. A.; Campbell, C. T. *Z. Phys. Chem.* **1997**, *198*, 169−187.
(15) Lamont, C. L. A.; Borbach, M.; Stenzel, W.; Conrad, H.; Bradshaw, A. M. *Chem. Phys. Lett.* **1994**, *230*, 265−270.
(16) Lamont, C. L. A.; Borbach, M.; Martin, R.; Gardner, P.; Jones, T. S.; Conrad, H.; Bradshaw, A. M. *Surf. Sci.* **1997**, *374*, 215−228.
(17) Pettiette-Hall, C. L.; Land, D. P.; McIver, R. T., Jr.; Hemminger, J. C. *J. Am. Chem. Soc.* **1991**, *113*, 2755.
(18) Land, D. P.; Pettiettehall, C. L.; McIver, R. T.; Hemminger, J. C. *J. Am. Chem. Soc.* **1989**, *111*, 5970−5972.
(19) Land, D. P.; Erley, W.; Ibach, H. *Surf. Sci.* **1993**, *289*, 237−246.
(20) Martin, R.; Gardner, P.; Tushaus, M.; Bonev, C.; Bradshaw, A. M. *J. Electron Spectrosc. Relat. Phenom.* **1990**, *54*/*55*, 773−778.
(21) Raval, R.; Chesters, M. A. *Surf. Sci.* **1989**, *219*, L505-L514.
(22) Xu, C.; Tsai, Y.-L.; Koel, B. E. *J. Phys. Chem.* **1994**, *98*, 585−593.
(23) Koel, B. E.; Blank, D. A.; Carter, E. A. *J. Mol. Catal. A*: *Chem.* **1998**, *131*, 39−53.
(24) Jiang, L. Q.; Koel, B. E. *J. Phys. Chem. Lett.* **1992**, *96*, 8694.
(25) Parker, D. H.; Pettiettehall, C. L.; Li, Y. Z.; McIver, R. T.; Hemminger, J. C. *J. Phys. Chem.* **1992**, *96*, 1888−1894.
(26) Sheppard, N. *Annu. Rev. Phys. Chem.* **1988**, *39*, 589.
(27) Chesters, M. A.; Gardner, P. *Spectrochim. Acta Part a-Mol. Biomol. Spectrosc.* **1990**, *46*, 1011−1015.
(28) Tsai, M.-C.; Friend, C. M.; Muertterties, E. L. *J. Am. Chem. Soc.* **1982**, *104*, 2539−43.
(29) Campbell, J. M.; Seimanides, S. G.; Campbell, C. T. *J. Phys. Chem.* **1989**, *93*, 815−826.
(30) Thomas, F. S.; Chen, N. S.; Ford, L. P.; Masel, R. I. *Surf. Sci.* **2001**, *486*, 1−8.
(31) Dilaria, P. A.; Petrie, W. T.; Vohs, J. M. *Appl. Surf. Sci.* **1997**, *115*, 243−251.
(32) Frank, M.; Bäumer, M. *Phys. Chem. Chem. Phys.* **2000**, *2*, 3723−3737.
(33) Haaland, D. M. *Surf. Sci.* **1981**, *111*, 555−574.
(34) Roberts, S.; Gorte, R. J. *J. Chem. Phys.* **1990**, *93*, 5337.
(35) Petrie, W. T.; Vohs, J. M. *J. Chem. Phys.* **1994**, *101*, 8098.
(36) Radulovic, P. V.; Feigerle, C. S.; Overbury, S. H. *J. Phys. Chem. B* **2000**, *104*, 3028−34.
(37) Ernst, K. H.; Ludviksson, A.; Zhang, R.; Yoshihara, J.; Campbell, C. T. *Phys. Rev. B* **1993**, *47* II, 13782−96.
(38) Yoshihara, J.; Campbell, J. M.; Campbell, C. T. *Surf. Sci.* **1998**, *406*, 235−245.
(39) Ludviksson, A.; Ernst, K. H.; Zhang, R.; Campbell, C. T. *J. Catal.* **1993**, *141*, 380−388.
(40) Campbell, C. T. *Surf. Sci. Rep.* **1997**, *227*, 1.
(41) Bäumer, M.; Freund, H.-J. *Prog. Surf. Sci.* **1999**, *61*, 127−198.
(42) Henry, C. R.; Chapon, C.; Giorgio, S.; Goyhenex, C. Size effects in heterogeneous catalysis: A surface science approach. In *Chemisorption and Reactivity on Supported Clusters and Thin Films*; Lambert, R. M., Pacchioni, G., Eds.; Kluwer Academic Publishers: Amsterdam, 1997; p 117.
(43) Henry, C. R. *Surf. Sci. Rep.* **1998**, *31*, 231.
(44) Parker, S. C.; Grant, A. W.; Bondzie, V. A.; Campbell, C. T. *Surf. Sci.* **1999**, *441*, 10−20.
(45) Starr, D. E.; Ranney, J. T.; Larsen, J. H.; Musgrove, J. E.; Campbell, C. T. *Phys. Rev. Lett.* **2001**, *8710*, art. no.-106102.
(46) Tersoff, J.; Tromp, R. M. *Phys. Rev. Lett.* **1993**, *70*, 2782.
(47) Grant, A. W.; Larsen, J. H.; Perez, C. A.; Lehto, S.; Schmal, M.; Campbel, C. T. *J. Phys. Chem.* **2001**, *105*, 9273−79.
(48) Venables, J. A. *Surf. Sci.* **1994**, *299*/*300*, 798.
(49) Venables, J. A.; Harding, J. H. *J. Cryst. Growth* **2000**, *211*, 27−33.
(50) Steinrück, H.-P.; Pesty, F.; Zhang, L.; Madey, T. E. *Phys. Rev. B* **1995**, *51*, 2427−2439.
(51) Wagner, C. D. *J. Elec. Spec. Relat. Phenom.* **1983**, *32*, 99.
(52) Tanuma, S.; Powell, C. J.; Penn, D. R. *Surf. Interface Anal.* **1991**, *17*, 911, 927.
(53) *CRC Handbook of Chemistry and Physics*, 77th ed.; Lide, D. R., Ed.; CRC Press: Boca Raton, FL, 1996.
(54) Ertl, G.; Küppers, J. *Low Energy Electrons and Surface Chemistry*; VCH: Weinheim, Germany, 1985.
(55) Diebold, U.; Pan, J.-M.; Madey, T. E. *Phys. Rev. B* **1993**, *47*, 3868−3876.
(56) Christmann, K.; Ertl, G.; Pignet, T. *Surf. Sci.* **1976**, *54*, 365−392.
(57) Greenlief, C. M.; Akhter, S.; White, J. M. *J. Phys. Chem.* **1986**, *90*, 4080−4083.
(58) Christmann, K. *Mol. Phys.* **1989**, *66*, 1−50.
(59) Firment, L. E.; Somorjai, G. A. *J. Chem. Phys.* **1977**, *66*, 2901.
(60) Redhead, P. A. *Vacuum* **1962**, *12*, 203.
(61) Ngo, L. T.; Grant, A. W.; Campbell, C. T. *J. Phys. Chem B* Submitted for publication.
(62) Zebisch, P.; Stichler, M.; Trischberger, P.; Weinelt, M.; Steinruck, H. P. *Surf. Sci.* **1998**, *396*, 61−77.
(63) Tsai, M.-C.; Muertterties, E. L. *J. Am. Chem. Soc.* **1982**, *104*, 2534−2539.
(64) Schauermann, S.; Hoffmann, J.; Johanek, V.; Hartmann, J.; Libuda, J. *Phys. Chem. Chem. Phys.* **2002**, *4*, 3909−3918.
(65) Ludviksson, A.; Zhang, R.; Campbell, C. T.; Griffiths, K. *Surf. Sci.* **1994**, *313*, 64−82.
(66) Zhang, R.; Ludviksson, A.; Campbell, C. T. *Catal. Lett.* **1994**, *25*, 277−292.
(67) Yoshihara, J.; Campbell, C. T. *Surf. Sci.* **1998**, *407*, 256−267.
(68) Campbell, J. M.; Campbell, C. T. *Surf. Sci.* **1989**, *210*, 46−68.